JOURNAL OF SOLID STATE CHEMISTRY 59, 1–8 (1985)

Crystal Structure, Luminescence, and Photoelectrochemistry of Thin Electroplated Cd-Chalcogenide Layers

M. ABRAMOVICH, M. J. P. BRASIL, F. DECKER, J. R. MORO, AND P. MOTISUKE

Instituto de Física, UNICAMP Caixa Postal 6165, 13.100 Campinas, SP, Brazil

N. MÜLLER-ST

Ophthalmology Department, Steglitz University Clinics, Hindenburgdamm 30, Berlin, West Germany

AND P. SALVADOR

Instituto de Catálisis y Petroleoquímica, CSIC, Serrano 119, Madrid, Spain

Received June 12, 1984; in revised form November 26, 1984

The relationship between crystal structure, photoluminescence spectrum, and photoelectrochemical behavior of $CdSe_xTe_{1-x}$ alloy layers has been investigated. Layers having the hexagonal wurzite structure are strongly luminescent both in the red (at a photon energy corresponding to the direct bandgap of the alloy) and in the near infrared. Much weaker luminescence is shown by the layers with cubic zincblende structure. Annealing is responsible for recrystallization and cubic-to-hexagonal phase transformation (CdSe-rich alloys), being beneficial to the efficiency both of photoluminescence and of photoelectrochemical solar energy conversion. © 1985 Academic Press, Inc.

1. Introduction

Electroplating is a cheap method to produce thin semiconducting films for application in solar energy conversion. CdSe and $CdSe_xTe_{1-x}$ are interesting materials, because their bandgap is in the optimal range for a photovoltaic cell (*1, 2*). A method for electroplating thin CdSe films was first reported in 1969 (*3*). More recently, electroplated CdSe and $CdSe_xTe_{1-x}$ alloy layers were used as semiconductor electrodes in photoelectrochemical (PEC) cells (*4, 5*). These devices are considered as possible candidates for economical solar energy conversion, since the charge-separating barrier is formed simply by immersion of the semiconductor electrode in a suitable electrolyte. Detailed studies have been undertaken (*5, 6*) in order to elucidate the growth mechanism of the CdSe layer both for galvanostatic and for potentiostatic

0022-4596/85 $3.00

electrodeposition conditions from a solution containing Cd^{2+} and SeO_2. Scanning electron micrographs of the plated electrodes show that the layers have irregular morphology being composed mostly of spherical particles ("cauliflower" morphology) (*4, 5*). This peculiar morphology (which is not observed to change with heat treatments) is believed to be ideal for a photoanode in the liquid junction solar cell configuration, since it leads to large effective contact area between semiconductor and electrolyte. Postdeposition heat treatment in a suitable atmosphere of the electroplated films is necessary prior to use in the PEC cell. After this treatment, the plated electrodes show high quantum efficiencies and reasonable stability in alkaline polysulfide electrolytes. Different annealing conditions have been reported in the literature in order to yield optimal solar cell performance (*4–6*), while the dependence of the physical and electrochemical parameters of the thin film electrodes on annealing temperature to our knowledge has not been published before.

Phase changes, recrystallization, and chemical composition changes may occur during annealing. The aim of the present work is to follow these chemical and structural transformations by X-ray diffraction and to correlate the structural properties to the optical properties of the films. We studied the photoluminescence (PL) spectra of the Cd-chalcogenide alloy layers. Room temperature PL of thin film II–VI compounds is very efficient (*7*) and the band-to-band radiative recombination allows the determination of the semiconductor bandgap. In addition, we correlate the general photoelectrochemical behavior of the electroplated layers annealed at different temperatures to their luminescence data. Particularly interesting is the comparison of the present results with literature data regarding the solid-state properties of single-crystal and polycrystalline homogeneous bulk materials (*1, 8, 9*).

2. Experimental Techniques

For preparing the thin film electrodes we followed the procedure given by Hodes *et al.* (*4*). Precleaned Ti substrates were immersed in one of the following plating baths: (A) 0.03 *M* SeO_2 + 0.2 *M* $CdSO_4$ + 1 *M* H_2SO_4; (B) 0.02 *M* SeO_2 + 0.01 *M* TeO_2 + 0.2 *M* $CdSO_4$ + 1 *M* H_2SO_4; (C) 0.006 *M* SeO_2 + 0.024 *M* TeO_2 + 0.2 *M* $CdSO_4$ + 1 *M* H_2SO_4. After 30 min of potentiostatic electrodeposition at a potential of −0.7 V (SCE) and at 25°C the electrodes were removed from the bath and carefully washed in water. The film thickness was of the order of a few micrometers. A plating bath volume of 0.5 liter was used, in which ten samples were immersed with cylindrical symmetry and electroplated simultaneously. This was found to be the best procedure in order to obtain identical layers. After plating the samples were annealed in a flowing stream of nitrogen or air for 15 min (each sample at a different temperature) and slowly cooled down to room temperature in the respective atmosphere. X-Ray powder diffractograms of the films were obtained using a Philips diffractometer with monochromatic Cu$K\alpha$ radiation, and KCl was used as an internal standard. For the determination of the lattice parameters five well-resolved peaks for the cubic phase and at least ten peaks for the hexagonal phase were considered and a least-squares method was employed. The crystal size in the (*hkl*) direction D_{hkl} was calculated from the Scherrer equation (*10*)

$$\beta_{cs} = \frac{K_\beta \lambda}{D_{hkl} \cos \theta}$$

where β_{cs} is the contribution to the experimental peak broadening due to the crystal size, K_β a constant close to unity, λ the wavelength, and θ the Bragg's angle. β_{cs} can be obtained from the measured peak width at half-height knowing the instrumental contribution to the peak broadening (from the (200) reflection of the NaCl stan-

dard) and applying Warren's rule (*10*). Room temperature PL spectra were taken in air with a 0.5-m SPEX spectrometer and a S-1-EMI photomultiplier cooled with liquid N_2. The 5145-Å line of a Coherent Radiation Model 52 Ar^+ ion laser was used to excite the luminescence. The laser beam was expanded to cover most of the electrode surface so that the intensity at the sample was about 100 mW/cm^2. The beam expansion was found to be important both to average the luminescence over a large sample area and to avoid local overheating with unintentional laser annealing at the beam spot. The polycrystalline $CdSe_xTe_{1-x}$ surfaces are quite inhomogeneous and the luminescence from a large sample area is much more reproducible than that from a narrow spot. Output–power curves in laboratory-type PEC cells with 2 *M* KOH/1.4 *M* Na_2S/2.6 *M* S electrolyte were measured by varying a load resistor between the photoelectrode and a brass counter electrode, as described elsewhere (*4*). A tungsten halogen lamp with a water filter was used as a light source to simulate solar AM2 illumination (75 mW/cm^2).

3. Experimental Results

3.1. X-Ray Diffraction

Table I shows the main crystallographic and composition data of the films obtained

TABLE I

CRYSTALLOGRAPHIC AND COMPOSITION DATA OF TYPICAL $CdSe_xTe_{1-x}$ FILMS, FROM X-RAY POWDER DIFFRACTOGRAMS

	Annealing (N_2)	Crystal phase	Grain size $D_{(110)}$ (Å)	Lattice constant (Å)	Composition ($CdSe_xTe_{1-x}$)
(A) 0.03 *M* SeO_2 + 0.2 *M* $CdSO_4$ + 1 *M* H_2SO_4	Without	ZB	100	a = 6.06	x = 1
	200°C	ZB + (W)	180	a = 6.06 a = 6.60	x = 1
	300°C	ZB + W	350	a = 4.30 a = 7.03	x = 1
	400°C	W	>5000	a = 4.30 c = 7.03	x = 1
(B) 0.02 *M* SeO_2 + 0.01 *M* TeO_2 + 0.2 *M* $CdSO_4$ + 1 *M* H_2SO_4	without	ZB	65	a = 6.19	x = 0.7
	200°C	ZB	65	a = 6.19 a = 6.19	x = 0.7
	400°C	ZB + (W)	140	a = 4.39 c = 7.19	x = 0.7
	500°C	W + (CdO)	240	a = 4.39 c = 7.20	x = 0.7
	600°C	W + (TiO_2)	390	a = 4.37 c = 7.12	x = 0.8
	700°C	W + (TiO_2)	>5000	a = 4.30 c = 7.02	x = 1
(C) 0.006 *M* SeO_2 + 0.024 *M* TeO_2 + 0.2 *M* $CdSO_4$ + 1 *M* H_2SO_4	without	ZB + (Cd)	70	a = 6.40	x = 0.2
	200°C	ZB + (Cd)	80	a = 6.37	x = 0.25
	350°C	ZB + (CdO)	130	a = 6.39	x = 0.2
	500°C	ZB + (CdO)	300	a = 6.35	x = 0.3
	600°C	ZB + (CdO)	570	a = 6.35	x = 0.3
	700°C	CdO + TiO_2	—	—	—

Note. ZB = zincblende cubic phase; W = wurzite hexagonal phase. Nominal composition is obtained from lattice constants by applying Vegard's law (*8*).

from the diffractograms, as a function of the annealing temperature and the chemical composition of the plating bath. From the unit-cell parameter we determine that the film compositions are CdSe, $CdSe_{0.7}Te_{0.3}$, and $CdSe_{0.2}Te_{0.8}$ for the layers plated in baths A, B, and C, respectively, as expected from the nominal bath compositions. The three films are found to have the cubic zincblende crystal structure. Traces of the hexagonal structure are found only for the CdSe samples. This hexagonal modification is known to be the more stable form for the CdSe-rich ternary alloys (*8*). The occurrence of the hexagonal phase is observed to increase with increasing annealing temperature for our CdSe and Cd $Se_{0.7}Te_{0.3}$ layers. Complete transformation to the hexagonal form is observed at 400°C for CdSe and at 500°C for $CdSe_{0.7}Te_{0.3}$. No transformation from the cubic to the hexagonal phase occurs under annealing for the $CdSe_{0.2}Te_{0.8}$ alloy; however, these layers disproportionate and after annealing a new phase of hexagonal $CdSe_{0.4}Te_{0.6}$ appears.

Prior to annealing, the grain size is less than 100 Å. Recrystallization occurs under heat treatment, as expected. However the recrystallization is slower for the $CdSe_x Te_{1-x}$ alloy than for the CdSe phase, since CdSe has already reached a great degree of crystallinity (crystal size of the order of several thousand angstroms) after annealing at 400°C, while this does not happen for the alloy even at 600°C. The crystal phase does not seem to affect the rate of recrystallization. Figure 1 summarizes the effect of annealing on the grain size of the electroplated layer for three different chemical compositions of the CdSeTe alloy. When the samples are annealed in air, complete oxidation of the layer takes place between 400 and 600°C. Diffraction peaks corresponding to metal oxides (mainly CdO and TiO_2) can also be detected in the diffractograms for temperatures above 500°C although annealing is performed under nitrogen, probably because of oxygen contamination.

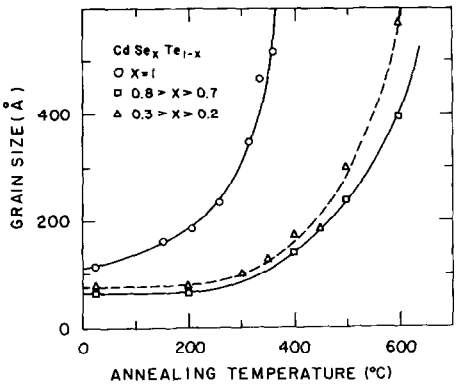

FIG. 1. Growth of the grain size as a function of annealing temperature, for three different alloy compositions (from X-ray diffraction data).

The existence of cadmium metal could also be expected since Cd^{2+} ions are in excess in the plating bath. However, this metal or its oxide is only detected in the films of the $CdSe_{0.2}Te_{0.8}$ alloy. As a general result the X-ray analysis shows that there is always somewhat more CdSe present in the alloy than expected from its nominal composition, particularly for high annealing temperatures. This phenomenon could be related to the sublimation of CdTe at high temperatures under atmospheric pressure.

3.2. Photoluminescence Spectra

The PL spectra of our electroplated samples were found to depend strongly on the crystal structure. Only the annealed layers with the wurzite structure show a well-defined peak in the red (720 nm for CdSe and 800 nm for $CdSe_{0.7}Te_{0.3}$), besides a broadband in the near infrared (1050 and 1090 nm for the binary and ternary compounds, respectively). The red emission at 720 nm of CdSe corresponds approximately to its bandgap energy of 1.7 eV (*11*). This is consistent with a description of the CdSe red PL as edge emission. The PL spectrum of the $CdSe_{0.7}Te_{0.3}$ is shifted toward infrared with respect to that of CdSe, in agreement

with the reported bandgap dependence on the alloy composition (*9*). The broadband in the infrared indicates the presence of states in the bandgap. Different and weaker luminescence is observed for layers with a predominantly zincblende structure. A single band peaking around 950 nm is always present for unannealed films, no matter the chemical composition of the alloy. Annealing does not change the shape of the PL spectrum unless it is accompanied by a phase transformation. As an example, all the samples from plating bath C shows approximately the same spectrum regardless of the annealing temperature. Among the samples with the wurzite structure the luminescence intensity increases with the annealing temperature. Log–log plots of the luminescence intensity versus the exciting light intensity yielded a slope less than 1 for the subbandgap luminescence and a slope 1 for the bandgap luminescence. Examples of the PL spectra for three different alloy compositions are shown in Figs. 2, 3, and 4.

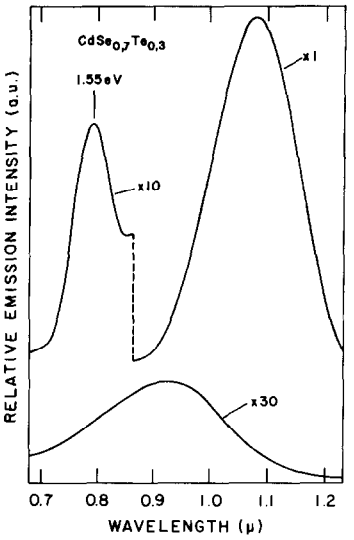

FIG. 3. Uncorrected photoluminescence of $CdSe_{0.7}Te_{0.3}$ thin layers: as-plated (lower curve) and after N_2 annealing at 600°C (upper curve). The composition of the annealed sample (from X-ray) is $CdSe_{0.8}Te_{0.2}$.

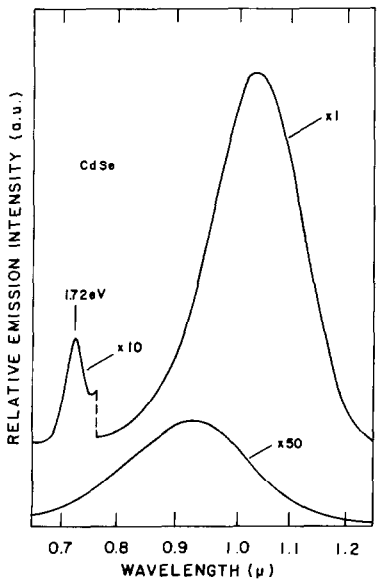

FIG. 2. Uncorrected photoluminescence of CdSe thin layers: as-plated (lower curve) and after N_2 annealing at 600°C (upper curve). Note scale changes.

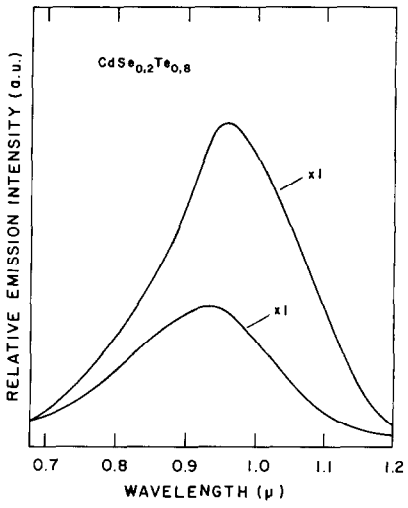

FIG. 4. Uncorrected photoluminescence of $CdSe_{0.2}Te_{0.8}$ thin layers: as-plated (lower curve) and after N_2 annealing at 600°C (upper curve). Both spectra are taken in the same scale and their intensity is comparable to that of the lower curves in Figs. 2 and 3. The composition of the annealed sample (from X-ray) is $CdSe_{0.3}Te_{0.7}$ + traces of $CdSe_{0.4}Te_{0.7}$.

3.3. Photoelectrochemical Behavior

The photocurrent–voltage curve of a CdSe thin film electrode in a polysuphide solution under simulated solar AM2 illumination before and after annealing is shown in Fig. 5. There is a drastic improvement of all the cell parameters (open circuit voltage, short circuit current, fill factor) and consequently of the cell conversion efficiency, which increases from 0.05 to 3%. Typical output parameters obtained with $CdSe_{0.7}Te_{0.3}$ photoelectrodes under 75 mW/cm² white light illumination are V_{oc} = 600 mV, I_{sc} = 15 mA/cm², and fill factor η = 40%. These data have not been corrected for reflection and electrolyte absorption losses. The improvement can be better followed studying samples which have been plated simultaneously, and annealed at different temperatures. In Fig. 6 we report the open-circuit photovoltage (V_{oc}) and the short-circuit photocurrent (I_{sc}) of several CdSe samples annealed in nitrogen between 300 and 700°C. First, a discontinuity is observed both for I_{sc} and V_{oc} at 400°C, which is the phase transformation temperature for CdSe. Second V_{oc} remains nearly constant for annealing temperatures larger than 450°C, while I_{sc} still increases monotonically. The fill factor shows a maximum (close to 40%) around 450°C. Similar results were obtained in experiments with a single electrode which had been successively annealed at increasing temperatures. Figures 5 and 6 show results for electrodes routinely obtained in our laboratory.

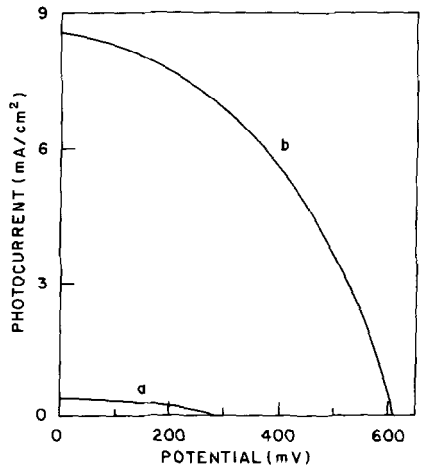

FIG. 5. Current–voltage curves of an illuminated (75 mW/cm²) 2-cm² CdSe thin film photoelectrode: (a) as-plated electrode; (b) after annealing at 640°C. Electrolyte 2 *M* KOH, 1.4 *M* Na_2S, 2.6 *M* S.

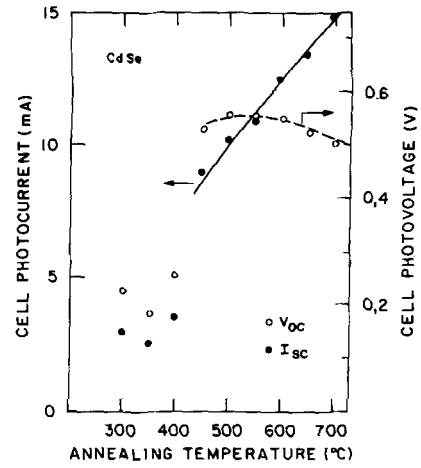

FIG. 6. Cell short-circuit photocurrent (I_{sc}) and open-circuit photovoltage (V_{oc}) of several CdSe layers plated simultaneously but annealed in N_2 at different temperatures. Electrode area = 2.5 cm². Illumination = 75 mW/cm²

Photoetching in a (0.3 : 9.7 : 90) $HNO_3 : HCl : H_2O$ solution under white light illumination and shortening the photoelectrode to a carbon counterelectrode; that is, a photoelectrochemical etching procedure producing an increase of the real surface area of the electrode and removal of surface recombination centers (*7, 12, 13*), improves both I_{sc} and V_{oc} by 10–20% but does not alter the general trend shown in Fig. 6. Since photoetching is exclusively a surface treatment, it is clear that the improvement in the cell parameters with annealing is related solely to changes in the bulk properties, such as crystal structure

and grain size of the thin electrodeposited layer.

4. Discussion and Conclusions

Our analysis confirms a previous report (*4*) that electroplated CdSe (and $CdSe_xTe_{1-x}$ where $x > 0.4$) exists in a metastable cubic zincblende structure that may change to hexagonal on annealing. For Te-rich alloys (where $x < 0.3$), on the other hand, the cubic form is the stable one. This is in agreement with earlier results on electroplated CdTe photoelectrodes (*14*). Haneman *et al.* (*15, 16*) found that as-deposited electroplated CdSe films were already hexagonal; however, their plating solution was an acid chloride bath. It has already been reported in the literature (*17*) that CdS obtained by precipitation of Cd^{2+} by H_2S is cubic in sulfate solution but hexagonal in chloride solution. Besides phase transformation, the effect of annealing is mainly that of recrystallization. In order to optimize the power output of PEC cells with these electrodes, the penetration depth of the light in the semiconductor should not exceed the grain size, as recombination at grain boundaries leads to significant losses in the conversion efficiency. Therefore the grain size should be at least 0.2 μm. This requirement is met for the alloy layers ($x < 1$) with annealing temperatures higher than 600°C, which obviously precludes the use of air as the annealing atmosphere. However, it has been reported that small quantities of oxygen in the annealing atmosphere are beneficial to the performance of such thin film electrodes (*1, 4*). Quite often we found small amounts of TiO_2 and CdO in the films even when annealing was performed under nitrogen. Small traces of oxygen therefore do oxidize the Ti substrate, probably improving the film adherence, and oxidize the excess of cadmium metal in the film, which would act as a recombination center.

The metastable cubic zincblende phase of CdSe does not show a good performance in the PEC cell (Figs. 5 and 6). The question is whether alloy layers with the cubic zincblende structure can also have good PEC behavior, as in the case of CdTe-rich alloys where high enough annealing temperature can be used without phase change. For instance Hodes *et al.* (*18*) found excellent results also for slurry painted $CdSe_{0.5}Te_{0.5}$ electrodes with cubic structure. Among our electroplated samples, however, the best results for solar conversion efficiency (6%) were reached with hexagonal $CdSe_{0.7}Te_{0.3}$ films, while the CdTe-rich electrodes had usually poor cell performances.

Photoluminescence provides an excellent optical method to characterize the material and its crystal structure. In this respect PL looks more convenient than the optical absorption measurement (*9*) which allow discrimination between the cubic and the hexagonal phase due to a slight (0.05 eV) displacement of the bandgap. Such a difference might be difficult to observe in an absorption spectrum or in a photocurrent spectrum of a rather impure material like that of our films. The luminescence spectra of the cubic and hexagonal phases, on the other hand, are completely different. The cubic zincblende form has a rather poor photoluminescence efficiency and shows a broadband at 950 nm regardless of the alloy composition (Figs. 2–4). The hexagonal wurzite form, on the contrary, is strongly luminescent both in the red and in the infrared. The infrared part of the spectrum (with maximum around 1.05 μm) is usually predominant. Subbandgap luminescence from CdS and CdSe single crystals to which no impurity has been intentionally added has been reported before (*19, 21*). Polycrystalline material like ours are expected to contain larger amounts of impurities and of structural defects than the single crystals (*22*). Several impurity states and cation–

anion vacancy associations are probably contributing simultaneously to the subbandgap luminescence (*23*). Low temperature luminescence studies are under way in order to separate different contributions. The red luminescence of CdSe and CdSe-rich alloys can be used to determine the bandgap of the material, provided it crystallizes with the hexagonal structure. Good agreement is found between our results (Figs. 2 and 3) and the optical bandgap reported in (*18*). A strong bandgap luminescence is usually an indication that the sample will be an efficient photoelectrode. Electrodes annealed at lower temperatures, for example, have a weak bandgap luminescence and poor short circuit photocurrent. Therefore PL can be used as a nondestructive dry selection test for Cd-chalcogenide photoelectrodes to be used in PEC cells.

In conclusion, we have demonstrated the possibility of plating a variety of $CdSe_x Te_{1-x}$ alloy layers with X ranging from 0.2 to 1. As-plated films have the cubic zincblende structure. Phase transformation eventually occurs upon annealing for CdSe-rich alloys. Such samples show strong red luminescence and optimal photocurrents after annealing around 650°C, which leads to complete cubic-to-hexagonal phase change and considerable recrystallization. A clear relationship between the crystallographic parameters and the luminescence spectra of the $CdSe_xTe_{1-x}$ thin films has been established.

Acknowledgments

The authors thank A. Lourenço and L. A. Santiago for their skillful technical assistance. The financial support from OEA, FINEP, CNPq, and the Ministerio de Educación y Ciencia de España is gratefully acknowledged.

References

1. G. Hodes, J. Manassen, and D. Cahen, *J. Amer. Chem. Soc.* **102,** 5962 (1980).
2. G. Hodes, J. Manassen, and D. Cahen, *Nature (London)* **261,** 403 (1976).
3. E. Paucauskas, J. Janickis, and A. Saudargaite, *Liet TSR Mokslu Akad. Darb. Ser. B* **4,** 75 (1969); *Chem. Abstr.* **72,** 85584c (1970).
4. G. Hodes, J. Manassen, S. Neagu, D. Cahen, and Y. Mirovsky, *Thin Solid Films* **90,** 433 (1982).
5. M. Tomkiewicz, I. Ling, and W. S. Parsons, *J. Electrochem. Soc.* **129,** 2016 (1982).
6. M. S. Kazacos and B. Miller, *J. Electrochem. Soc.* **127,** 869 (1980).
7. N. Müller, M. Abramovich, F. Decker, F. Iikawa, and P. Motisuke, *J. Electrochem. Soc.* **131,** 2204 (1984).
8. A. S. Stuckes and G. Farrel, *J. Phys. Chem. Solids* **25,** 477 (1964).
9. H. Tai, S. Nakashima, and S. Hori, *Phys. Status Solidi A* **30,** 115 (1975).
10. L. V. Azaroff, "Elements of X-Ray Crystallography," p. 549, McGraw–Hill, New York (1968).
11. R. G. Wheeler and J. Dimmock, *Phys. Rev.* **125,** 1805 (1962).
12. R. Tenne and G. Hodes, *Appl. Phys. Lett.* **37,** 428 (1980).
13. N. Müller and R. Tenne, *Appl. Phys. Lett.* **39,** 283 (1981).
14. M. P. R. Panicker, M. Knaster, and F. A. Kröger, *J. Electrochem. Soc.* **125,** 566 (1978).
15. D. J. Miller and D. Haneman, *Solar. Energy Mater.* **4,** 223 (1980).
16. D. Haneman *et al.*, *Solar Energy Mater.* **4,** 232 (1980).
17. H. Hartmann, *Kristallogr. Technol.* **1,** 267 (1966).
18. G. Hodes, D. Cahen, J. Manassen, and M. David, *J. Electrochem. Soc.* **127,** 2252 (1980).
19. M. K. Sheinkman, I. B. Ermilovich, and G. I. Belen' Kú, *Sov. Phys. Solid State* **10,** 2069 (1969).
20. H. H. Streckert, J. Tony, M. K. Carpenter, and A. B. Ellis, *in* "Proceedings of the Symposium on Photoelectrochemistry" p. 633, Electrochem. Soc., Pennington, N.J. (1982).
21. C. B. Norris, *J. Appl. Phys.* **53,** 5177 (1982).
22. B. J. Feldman and J. A. Duisman, *Appl. Phys. Lett.* **37,** 1092 (1980).
23. C. N. Elsby and J. M. Meese, *J. Appl. Phys.* **43,** 4818 (1972).